Asian Journal of Chemistry; Vol. 29, No. 3 (2017), 661-664

ASIAN JOURNAL OF CHEMISTRY

https://doi.org/10.14233/ajchem.2017.20297

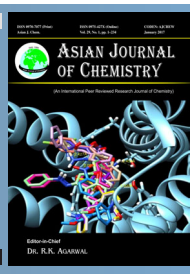

Structural and Microstructural Properties of Nanostructured PLZT (9/60/40) Electroceramics Synthesized by Mechanical Alloying Process

MOHAMMAD HOSSEIN GOLMAKANI[1,*], MOHAMMAD REZA GHAZANFARI[2], YOUNES LAGZIAN[2], SEYYEDEH FATEMEH SHAMS[2] and RASOOL AMINI[3]

[1]Department of Materials Engineering and Ceramic, Mashhad Branch, Islamic Azad University, Mashhad, Iran
[2]Department of Materials Science and Engineering, Ferdowsi University of Mashhad, 9177948974, Mashhad, Iran
[3]Department of Materials Science and Engineering, Shiraz University of Technology, Shiraz, Iran

*Corresponding author: E-mail: Hos.glgh@gmail.com; hgol617@yahoo.com

Received: 9 September 2016; *Accepted*: 25 November 2016; *Published online*: 30 December 2016; AJC-18222

In current work, the $(Pb_{91}La_9)(Zr_{60}Ti_{40})O_3$ electroceramic known as PLZT (9/60/40) was synthesized by mechanical alloying technique. The chemical composition assessments and structural properties of milled samples at different milling time were studied by X-ray fluorescence (XRF) and X-ray diffraction (XRD) analyses. Moreover, the structural evaluations were carried out by scanning electron microscope and transmission electron microscope. The X-ray fluorescence results showed that the chemical compositions of milled powder had negligible deviation from stoichiometric ratio. The mechanism of PLZT synthesis by mechanical alloying had three steps include (a) the crystallite size decreasing of initial materials to nanometer scales, (b) amorphous phase formation and (c) the recrystallization of perovskite structure from amorphous phase. Furthermore, by increasing of milling time the particles size was gradually decreased to about 20 nm in 40 h milled sample and their morphology was transformed from irregular shape to equiaxed quasi-spherical mode.

Keywords: Ceramics, Electron microscopy, Microstructure, Piezoelectricity.

INTRODUCTION

Generally, the electroceramic materials with perovskite structure have been mostly considered due to their appropriate piezoelectric, pyroelectric, ferroelectric and electro-optic properties [1-5]. One of the most common groups of these materials is the lead zirconium titanate (PZT) based ceramics which are found the special importance in electronic and microelectronic technologies because of their unique electronic behaviors [1-8]. The $(Pb_xLa_{1-x})(Zr_yTi_{1-y})O_3$ compositions can be utilized in many improved advance applications [2-5]. In fact, the presence of La in these compositions is led to develop some new properties such as increasing of dielectric Curie temperature [owing to broadening of diffusion phase transformation (DPT) region], increasing of polarization-electric field (PE) hysteresis loop area, decreasing of coercive field (Hc), dielectric constant improvement, coupling coefficient augmentation and creation of optical transparency [9-12]. The variation of optical transparency is formed by Pb^{2+} substitution by La^{3+} while the radius and optical coefficients of these ions are diverse because of their different electron configuration and interactions [9-14]. Accordingly, the special optical properties of $(Pb_{91}La_9)(Zr_{60}Ti_{40})O_3$ (PLZT) are caused to considerable performance in various applications *i.e.* sensors, transducers, and optical memories [12-14]. Based on different stoichiometries of PLZT, the Zr/Ti ratio and amount of doped La can significantly effect on the final behaviours of structure [2-5]. According to PLZT phase diagram, it can be concluded that in order to achieve the optimum conditions including suitable piezoelectric, dielectric and optic properties, the stoichiometric compositions on the morphotropic phase boundary (MPB) region of tetragonal-rhombohedral phases are most appropriate [1-5]. Hence, this condition can be attained when Zr/Ti ratio is selected equal to 60/40 (%). Furthermore, the Pb substitution by 8 % ≤ La is led to improve the optical transparency of samples [9-11]. As a result, the $(Pb_{91}La_9)(Zr_{60}Ti_{40})O_3$ known as PLZT (9/60/40) can present the considerable properties especially in sensor and optical memory applications.

In electroceramics like PLZT, the achievement of high density plays significant role in order to improve desired properties [14]. The most common method of PLZT synthesis is the conventional mixed oxide that requires a high temperature (900-1000 °C) calcination process [12-14]. Considering evaporation of Pb compounds at about 800 °C, the high temperature calcination can be caused to aberration from stoichiometric ratio and decreasing properties [14]. Moreover, in this method,

in order to achieve appropriate properties, high temperature and time-consuming heating processes (calcination and sintering) are necessary. Thus, the production cost is augmented. Although the other synthesis methods like wet chemical techniques *i.e.* sol-gel, coprecipitation and hydrothermal can be utilized for the synthesis of higher density nano-structured PLZT powder. Owing to expensive required raw materials, toxicity of some agents and relatively complex processes these techniques are rarely employed in industrial scales compared to conventional method [1,5,14].

The mechanical alloying (MA) method is one of the efficient fabrication approaches of nanostructured electroceramics powder like PZT and PLZT. The main advantages of this method include low cost raw materials, simple and non-toxic process, decreasing of calcination and sintering temperatures and times, higher final density of samples, reducing of deviation in stoichiometry that is caused by Pb evaporation and properties improvement [15-19].

Accordingly, in current work, the main efforts are focused on the synthesis of nanostructured PLZT (9/60/40) powders by mechanical alloying process, investigation of alloying mechanisms during process and study of their structural and microstructural properties.

EXPERIMENTAL

In order to synthesize PLZT compound, the initial materials consisting of TiO_2 (Merck, > 99.5 %), PbO (Merck, > 99 %), La_2O_3 (Merck, > 99.5 %) and ZrO_2 (Merck, > 99.5 %) were mixed in agate mortar according to PLZT (9/60/40) stoichiometric ratio. Subsequently, the mixture was milled in dry conditions under air atmosphere by use of planetary ball mill (Sepahan 84D) with a tempered steel cup (capacity: 80 ml) at the rotation speed of 200 rpm (disk to cup rotation speeds ratio was 2:1) while the tempered steel balls consisting of four balls with diameter of 20 mm and seven balls with diameter of 10 mm. Furthermore, the ball to powder ratio was selected equal to 20:1. During process, samples were obtained at different milling times from 5 to 40 h. In order to evaluate the variation of chemical compositions of as-milled powders and probable contaminations, the X-ray florescence analyses were done by XRF (Philips, PW2400) based on extraction of quantitative values using PAN analytical software. The structural properties of samples were studied by X-ray diffraction analysis using XRD (Bruker Advance 2) in the 2θ range of 20° to 60° with a step size of 0.05° and step time of 4 s. The XRD tests were performed at room temperature with the operation condi-tions of Cu $K_{\alpha 1,2}$ radiation at 40 kV and 40 mA. Moreover, the microstructural evaluations such as particles size and morphology were carried out by scanning electron microscope (SEM, JEOL-JSM 6349F) and transmission electron microscope (TEM, JEOL 2010).

RESULTS AND DISCUSSION

Chemical composition assessment: One of the most important goals of the using mechanical alloying process to synthesize PLZT powders is the declination of Pb evaporation, thereby decreasing the deviation from stoichiometric composition. Table-1 indicates the chemical composition of the as-milled sample for 40 h. based on these results, it is clear that the Pb amount in sample composition was corresponded to the initial stoichiometric ratio. In fact, PLZT powders synthesized by mechanical alloying method showed negligible deviation from nominal composition. In addition, considering the composition and milling time the amounts of some critical contaminations including Fe and Cr (because of using tempered steel cup and balls) were considerably low. The reason of these negligible amounts can be known as the creation of an adhesive layer of powders on the surface of cup and balls in initial milling times.

Accordingly, it can be concluded the mechanical alloying process and selected milling conditions were suitable to fabricate PLZT compounds.

Structural properties: Fig. 1 illustrates the XRD patterns of the powders as a function of different milling times. According to these results, it can be observed that positions and intensity of peaks were varied by milling time augmentation. In the pattern of 5 h milled sample, the peaks of La_2O_3 were completely disappeared while the intensity of TiO_2 phase peaks was relatively decreased due to their low initial amounts. On the other hand, the peaks intensity and broadening of α-PbO and ZrO_2 were grown and reduced, respectively. The sensible presence of these phases peaks compared to La_2O_3 and TiO_2 can be related to higher initial amounts and higher melting point (in the case of ZrO_2) [20-23]. Furthermore, in this pattern, in can be seen no perovskite peaks of PLZT structure. By the milling evaluation to 10 h, the abatement of intensity and sharpness was continued while the peaks broadening was amplified as a result of the decrement of crystallite size of initial phases, increment of lattice micro-strain of these phases, and formation of amorphous phase [20-22]. Moreover, it can be observed that the peaks locations were shifted to lower degrees owing to increase the distance between atomic planes that was caused by micro-strain augmentations in structures [20-26]. Additionally, the high angle peaks (2θ > 50°) were relatively disappeared because of high amorphous phase [20-22]. The XRD pattern of 20 h milled sample demonstrates no sharp peaks which can be explained by the presence of high amount of amorphous phase. In fact, the increase in milling process up to 10 h was caused to further transformation of initial phases to amorphous structure. Finally in pattern of 40 h milled sample, the sharp peaks of perovskite structure are clearly observed which indicate the formation of PLZT phase. Moreover, the peaks of initial materials were entirely vanished.

TABLE-1
CHEMICAL COMPOSITION OF THE 40 h MILLED SAMPLE

Milling time (h)	Weight (%)													
	Pb		La		Zr		Ti		O		Cr		Fe	
	Conc.	AE	Conc.	AE	Conc.	AE	Conc.	AE	Conc.	AE	Conc.	AE	Conc.	AE
40	58.338	0.071	3.861	0.016	16.814	0.056	5.821	0.021	14.732	0.041	0.084	0.003	0.052	0.002

Conc. = Concentration; AE = Absolute error

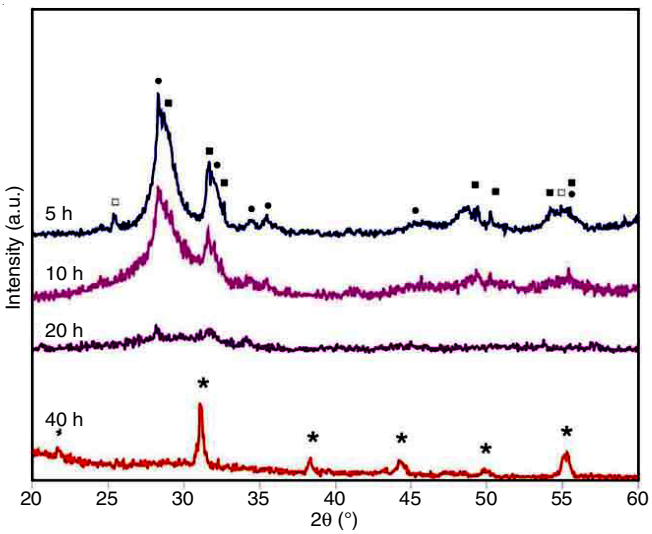

Fig. 1. XRD patterns of the powders as a function of different milling times. It is clear that by increasing milling time, the sharpness of initial phases is decreased, the amorphous phase is developed, and finally the PLZT structure is re-crystallized from amorphous phase. [Notations: ZrO_2 (●), TiO_2 (□), α-PbO (■) and Perovskite structure of PLZT (*)]

According to results, it can be concluded that the PLZT creation mechanism has three critical steps including (a) crystallite size decreasing and micro-strain increasing of initial phases, (b) formation and development of amorphous phase, and (c) recrystallisation of PLZT perovskite structure from amorphous phase. In fact, in mechanical alloying method, by employing mechanical energy instead of thermal energy as a motivation of required chemical reactions, the PLZT powders were achieved without any heat treatment process like calcination; thus the final structure showed negligible deviation from stoichiometric ratio. On the other word, in mechanical alloying process, by use of non-equilibrium conditions, due to the dislocations interaction and lattice strain increase, the desired structure can form in lower temperature [26-30]. Furthermore, during mechanical alloying, besides applied mechanical energy the local temperature augmentation can be occurred by collisions of walls, balls, and powders to each other [28-30]. Accordingly, it can be expected that the sintering process of synthesized powders by mechanical alloying requires lower time and temperature.

Microstructural evaluations: Fig. 2 demonstrates the SEM micrographs of milled samples at different milling times. Based on these images, it is clear that by increasing of milling time the particles size was gradually decreased and their morphology was transformed from irregular shape to equiaxed quasi-spherical mode. Moreover, the investigations of size variations by image analyzer software showed that in the 40 h milled sample, the average particle size was equal to 110 nm with ranging from 30 to 800 nm. In order to study precisely the microstructural properties, the microscopic observation were utilized. Fig. 3 shows the TEM micrograph of 40 h milled powders that indicates the creation of semi-spherical particles with average size of 21 nm with ranging of 8 to 44 nm. The main reason of difference between SEM and TEM results is caused by presence of considerable agglomeration in SEM samples [20]. Table-2 lists the variations of particles size as a function of milling time that is resulted from TEM analyses. Based on these results, initially the particles size was rapidly decreased and then was gradually reduced by increasing of mechanical alloying process. In fact, in first stages of mechanical alloying owing to fracture mechanism of brittle structures, the decreasing of particles size was occurred quickly. However,

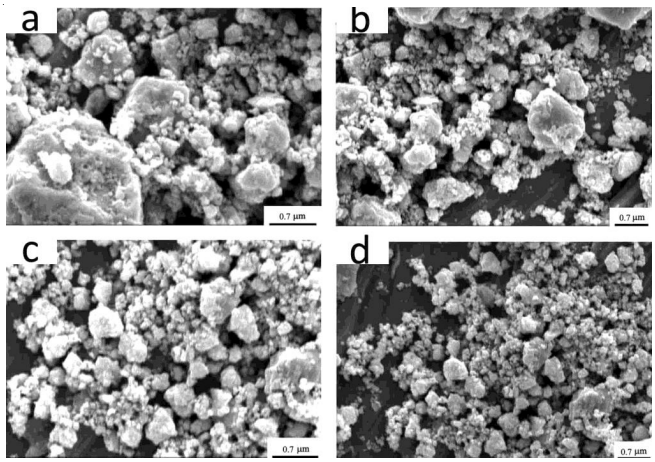

Fig. 2. SEM micrographs of milled samples at (a) 5 h, (b) 10 h, (c) 20 h and (d) 40 h milling time. By milling time augmentation, the particles size was gradually decreased and their morphology was transformed from irregular shape to equiaxed quasi-spherical mode

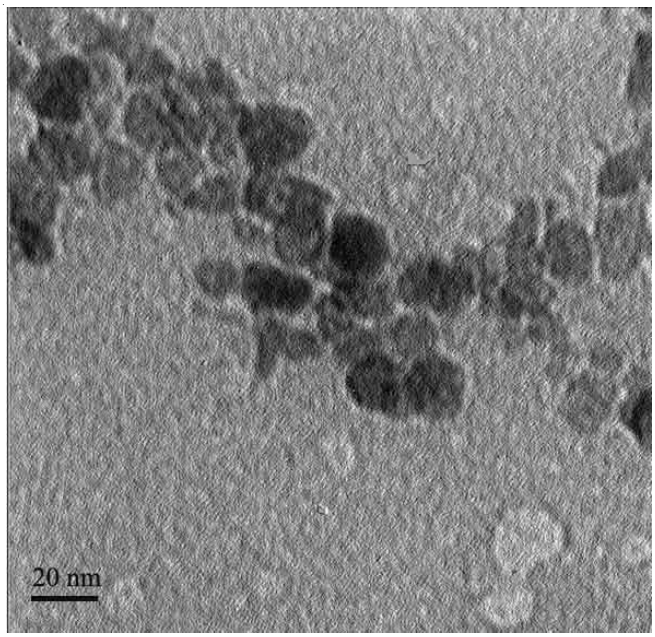

Fig. 3. TEM micrograph of 40 h milled sample that indicates the creation of semi-spherical particles with average size of 21 nm with ranging of 8 to 44 nm

TABLE-2
VARIATION OF PARTICLES SIZE AS A FUNCTION OF MILLING TIME *i.e.* RESULTED FROM TEM ANALYSES

Milling time (h)	Particle size (nm)	
	Minimum	Maximum
0	146	449
5	59	127
10	37	79
20	19	57
40	8	44

by mechanical alloying progress to critical threshold, the particles fracture mechanism is changed from brittle mode to ductile state, and the successive fracture and cold welding process were occurred in powders which are led to gradient decrement of particles size reduction [21,31].

Conclusion

In this research, the $(Pb_{91}La_9)(Zr_{60}Ti_{40})O_3$ composition known as PLZT (9/60/40) was successfully synthesized by mechanical alloying technique using the raw materials consisting of TiO_2, La_2O_3, ZrO_2 and PbO. Furthermore, in order to study the synthesis mechanism, the structural and microstructural of as-milled samples were carried out which are led to conclude some results. By increasing of milling time, the intensity and broadening of initial materials were reduced and augmented, respectively in first stages. Then, the amorphous phase was developed from initial materials and afterwards by mechanical alloying progression up to 40 h the perovskite structure of PLZT phase was created. In fact, the synthesis mechanism of PLZT by mechanical alloying had three steps include:

(a) The crystallite size decreasing of initial materials to nanometer scales

(b) Amorphous phase formation

(c) Recrystallization of perovskite structure from amorphous phase. Moreover the microstructural investigations show that by increasing of milling time the particles size was gradually decreased to about 20 nm in 40 h milled sample and their morphology was transformed from irregular shape to equiaxed quasi-spherical mode. The particle size decreasing was occurred rapidly in short milling times while by mechanical alloying development the gradient of this variation was reduced owing to transformation of particles fracture mechanism from brittle to ductile modes.

REFERENCES

1. J.F. Li, K. Tatagi and B.P. Zhang, *J. Mater. Sci.*, **39**, 2879 (2004).
2. K. Takagi, J.F. Li and R. Watanabe, *KONA Powd. Part.*, **21**, 234 (2003).
3. A.R. James and J. Subrahmanyam, *J. Mater. Sci. Mater. Electron.*, **17**, 529 (2006).
4. L.B. Kong, J. Ma, W. Zhu and O.K. Tan, *J. Mater. Sci. Lett.*, **19**, 1963 (2000).
5. R.F. Elhajjar and S.S. Shams, *Polym. Test.*, **35**, 45 (2014).
6. S.S. Shams and R.F. El-Hajjar, *Int. J. Mech. Sci.*, **67**, 70 (2013).
7. S.S. Shams and R.F. El-Hajjar, *Compos., Part A Appl. Sci. Manuf.*, **49**, 148 (2013).
8. G. Cocco, F. Delogu and L. Schiffini, *J. Mater. Synth. Process.*, **8**, 167 (2000).
9. A.R. James, B.S.S. Chandra Rao, S.V. Kamat, J. Subrahmanyam, K. Srinivas and O.P. Thakur, *J. Smart Mater. Struct.*, **17**, 035020 (2008).
10. K. Takagi, S. Kikuchi, J.F. Li, H. Okamura, R. Watanabe and A. Kawasaki, *J. Am. Ceram. Soc.*, **87**, 1477 (2004).
11. I. Szafraniak-Wiza, B. Hilczer, E. Talik, A. Pietraszko and B. Malic, *Process. Appl. Ceram.*, **4**, 99 (2010).
12. L.B. Kong, J. Ma, R.F. Zhang and T.S. Zhang, *J. Alloys Comp.*, **339**, 167 (2002).
13. Y. Zhang, A.L. Ding, P.S. Qiu, X.Y. He, X.S. Zheng, H.R. Zeng and Q.R. Yin, *Mater. Sci. Eng.*, **99**, 360 (2003).
14. L.B. Kong, T.S. Zhang, J. Ma and F. Boey, *Prog. Mater. Sci.*, **53**, 207 (2008).
15. L.B. Kong, J. Ma, H. Huang and R.F. Zhang, *J. Alloys Comp.*, **345**, 238 (2002).
16. L.B. Kong, J. Ma, W. Zhu and O.K. Tan, *Mater. Res. Bull.*, **36**, 1675 (2001).
17. L.B. Kong, J. Ma, W. Zhu and O.K. Tan, *J. Alloys Comp.*, **322**, 290 (2001).
18. C. Miclea, C. Tanasoiu, A. Gheorghiu, C.F. Miclea and V. Tanasoiu, *J. Mater. Sci.*, **39**, 5431 (2004).
19. R. Amini, M.R. Ghazanfari, M. Alizadeh, H.A. Ardakani and M. Ghaffari, *Mater. Res. Bull.*, **48**, 482 (2013).
20. R. Amini and M.R. Ghazanfari, *J. Alloys Comp.*, **587**, 520 (2014).
21. H.A. Ardakani, M. Alizadeh, R. Amini and M.R. Ghazanfari, *Ceram. Int.*, **38**, 4217 (2012).
22. M. Alizadeh, H.A. Ardakani, R. Amini, M.R. Ghazanfari and M. Ghaffari, *Ceram. Int.*, **39**, 3307 (2013).
23. J. Lappalainen, J. Puustinen, J. Hiltunen and V. Lantto, *J. Eur. Ceram. Soc.*, **30**, 497 (2010).
24. S. Yang, Y. Zhang and D. Mo, *Mater. Sci. Eng. B*, **127**, 117 (2006).
25. R. Amini, M.J. Hadianfard, E. Salahinejad, M. Marasi and T. Sritharan, *J. Mater. Sci.*, **44**, 136 (2009).
26. Z. Zheng, X. Li, J. Liu, Z. Feng, B. Li, J. Yang, K. Li, H. Jiang, X. Chen, J. Xie and H. Ming, *J. Phys. B*, **403**, 44 (2008).
27. G.H. Haertling and C.E. Land, *J. Am. Ceram. Soc.*, **54**, 1 (1971).
28. K. Kitaoka, H. Kozuka and T. Yoko, *J. Am. Ceram. Soc.*, **81**, 1189 (1998).
29. D. Kuscer, E.T. Sturm, J. Kovac and M. Kosec, *J. Am. Ceram. Soc.*, **92**, 1224 (2009).
30. C. Suryanarayana, Mechanical Alloying and Milling, CRC Press, New York (2004).
31. J. Karch, R. Birringer and H.J. Gleiter, *Nature*, **330**, 556 (1987).